MIT Open Access Articles

Development of Cr cold spray–coated fuel cladding with enhanced accident tolerance

Original Article

Development of Cr cold spray–coated fuel cladding with enhanced accident tolerance

Martin Ševeček [a, b, *], Anil Gurgen [a], Arunkumar Seshadri [a], Yifeng Che [a], Malik Wagih [a], Bren Phillips [a], Victor Champagne [c], Koroush Shirvan [a]

[a] Department of Nuclear Science and Engineering, Massachusetts Institute of Technology, Cambridge, MA, USA
[b] Faculty of Nuclear Sciences and Physical Engineering, Czech Technical University in Prague, Prague, Czech Republic
[c] ARL Cold Spray Center, U.S. Army Research Laboratory, Aberdeen, MD, USA

ARTICLE INFO

ABSTRACT

Accident-tolerant fuels (ATFs) are currently of high interest to researchers in the nuclear industry and in governmental and international organizations. One widely studied accident-tolerant fuel concept is multilayer cladding (also known as coated cladding). This concept is based on a traditional Zr-based alloy (Zircaloy-4, M5, E110, ZIRLO etc.) serving as a substrate. Different protective materials are applied to the substrate surface by various techniques, thus enhancing the accident tolerance of the fuel. This study focuses on the results of testing of Zircaloy-4 coated with pure chromium metal using the cold spray (CS) technique. In comparison with other deposition methods, e.g., Physical vapor deposition (PVD), laser coating, or Chemical vapor deposition techniques (CVD), the CS technique is more cost efficient due to lower energy consumption and high deposition rates, making it more suitable for industry-scale production. The Cr-coated samples were tested at different conditions (500°C steam, 1200°C steam, and Pressurized water reactor (PWR) pressurization test) and were precharacterized and postcharacterized by various techniques, such as scanning electron microscopy, Energy-dispersive X-ray spectroscopy (EDX), or nanoindentation; results are discussed. Results of the steady-state fuel performance simulations using the Bison code predicted the concept's feasibility. It is concluded that CS Cr coating has high potential benefits but requires further optimization and out-of-pile and in-pile testing.

© 2018 Korean Nuclear Society, Published by Elsevier Korea LLC. This is an open access article under the CC BY-NC-ND license (http://creativecommons.org/licenses/by-nc-nd/4.0/).

1. Introduction

Current nuclear fuel systems for light water reactors (LWRs) are based on a combination of a slightly enriched UO_2 pellet and a cladding made of a Zr-based alloy. This system has been used for about half a century, and its safety and performance have been continuously improved and optimized. However, rare events have occurred in which this system does not behave as safely as desired. These events include the accident at the Three Mile Island, TMI-2 reactor in 1979 and the severe events at Fukushima Daiichi in 2011. After the Fukushima accident, the nuclear industry, utilities, and research and governmental organizations started R&D programs with the objective of development of a nuclear fuel system with enhanced accident tolerance or development of accident-tolerant fuels (ATF).

One of the widely studied ATF concepts is multicomponent cladding (also known as coated cladding). The cladding is considered a near-term technology that can be developed and employed in several years. The concept is based on modification of current Zr-based alloys, on which different protective layers are deposited. Many coating materials have been studied by different groups, including different deposition techniques. This article summarizes results of testing of Zircaloy-4 (Zry-4) cladding coated with chromium using cold spray (CS) technique. Similar cladding concepts are under development at CEA/AREVA [1], Korea Atomic Energy Research Institute [2], Westinghouse Electric Company [3], Czech Technical University [4], Ukraine [5], Institute for Energy Technology [6,7], and other institutes.

2. Materials and methods

2.1. Material and sample preparation

Chromium was chosen as a coating material mainly due to its extraordinary corrosion resistance, high melting point, good

* Corresponding author. Department of Nuclear Science and Engineering, Massachusetts Institute of Technology, Cambridge, MA, USA.
E-mail addresses: martin.sevecek@fjfi.cvut.cz, sevecek@mit.edu (M. Ševeček), agurgen@mit.edu (A. Gurgen), arunmdm@mit.edu (A. Seshadri), yfche@mit.edu (Y. Che), mwagih@mit.edu (M. Wagih), bren@mit.edu (B. Phillips), victor.k.champagne.civ@mail.mil (V. Champagne), kshirvan@mit.edu (K. Shirvan).

strength, high hardness, and good wear resistance. At the same time, chromium does not have a high neutron absorption cross section relative to natural elements such as nickel and is widely available at a reasonable cost. Owing to their similar mechanical and thermal properties, chromium is expected to be compatible with Zr-based alloys up to their eutectic temperatures, which are summarized in Table 1. Moreover, operating experience with chromium inside reactor cores already exists because control rods in some LWRs were plated with chromium to increase wear resistance; chromium is also an alloying element in core structural steels.

Standard commercially available annealed Zry-4 was used as a substrate. The composition of the substrate as provided by the supplier and confirmed by EDX was the following: 1.32Sn-0.21Fe-0.11Cr-0.13O-BalZr. The Zry-4 material was cleaned, descaled, and handled before different experiments following the ASTM standard [8].

2.1.1. Cold spray process

Zr-based substrate materials coated with chromium using various deposition methods have been widely studied [5,12,13]; however, the CS technique brings new questions and uncertainties to the ATF development process that have to be further investigated. The CS process involves the acceleration of micron-sized particles (~5—75 μm) in the form of commercially available powders that are carried at a high pressure (6.8 bar/100 psi—69 bar/1,000 psi) and sometimes in a heated gas stream (RT—1,200°C) in the solid state toward a suitable substrate, upon which the particles undergo tremendous plastic deformation [14].

Upon impact, the plastic deformation disrupts and breaks down surface oxide layers on both the powder and the substrate, leading to a metallurgical bond and mechanical interlocking [15]. Because the feedstock powder is deposited in the solid state, the microstructure is retained after deposition, with the exception of dynamic recrystallization due to high strain levels. The CS process is good for materials that can not only undergo high levels of strain with low energy input but are also sufficiently work hardened to obtain the desired strength. An impact-induced shock wave interacts with the expanding contact edge of an impacting particle [16], followed by adiabatic shear localization during the high-speed deformation of the particles on impact; this impact is characterized by localized temperature increases and strain concentration. Approximately 90% of the work of plastic deformation is converted to heat; the flow stress of most metals is sensitive to temperature, decreasing as temperature increases. During impact of the solid feedstock powder particles, the oxide layers on both the powder and the substrate surface are disrupted by "jetting" of the material and are partially removed, along with other impurities at the particle—substrate interface, exposing highly reactive "virgin" metal

and inducing subsequent metallic bonding between particle and substrate material [17]. The feedstock powder is in intimate contact with the exposed substrate, forming an adherent metallurgical bond as a result of the severe plastic deformation during particle impact [18]. Therefore, it can be deduced based on empirical evidence that impact-induced shock wave and adiabatic shear, in combination with mechanical interlocking, serve as predominant bonding mechanisms in CS.

The bonding mechanism associated with CS is analogous to that of cold welding, which is another type of solid phase welding process in which bonding is also the result of plastic deformation of the metals to be bonded. Bonding occurs at the "critical impact velocity" when two surfaces under extreme pressure are forced together such that the surface oxide layers are disrupted and bonding takes place between the opposing virgin metal surfaces [19]. Evidence from single particle impact experiments shows that the critical velocity of specific materials and the phenomenon of jetting are closely linked to shock-compaction phenomena [20].

The VRC Gen III high-pressure CS system was used to produce all the specimens and was operated using helium as the accelerating gas. The feedstock powder was pure chrome (Fig. 1), produced by Exotech, USA, and had an average particle size of 44 μm, an oxygen content of 600 ppm, and a nano-hardness value of 5.1 GPa. A De Laval tungsten carbide nozzle with a circular exit was used for this study. It has a 0.068-inch (1.75 mm) throat, a 0.2-inch (5 mm) exit with a 6-inch (152 mm) expanding length, and a 10° converging section. The remaining process conditions are listed in Table 2. The as-coated surface without any additional treatment is shown in Figs. 2 and 3.

2.2. 500°C steam oxidation test

Samples were first tested in low temperature steam to simulate in-reactor corrosion of the cladding material. The choice of the steam testing temperature results from a compromise between the
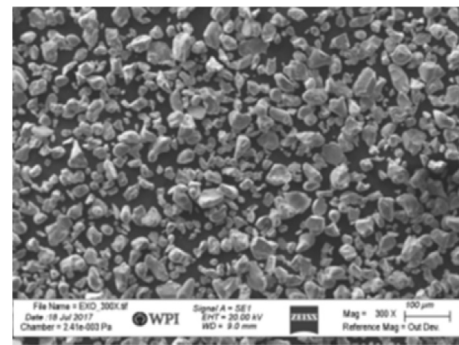

Fig. 1. SEM of the feedstock chrome powder produced by Exotech. SEM, scanning electron microscopy.

Table 1
Properties of substrate and coating materials at room temperature [9—11].

Material property	Chromium	Zircaloy-4
Ultimate tensile strength [MPa]	413	517
Yield strength [MPa]	362	348
Young's modulus [GPa]	140	99.3
	(PVD coating)	
Elongation[%]	0%	23%
Poisson ratio	0.21	0.37
Coefficient of thermal expansion [μm/m-°C]	6.20	6.00
Thermal conductivity [W/m-K]	69.1	21.5
Melting point/Eutectic [°C]	1860/1310	1850/1310
Specific heat capacity [J/g-°C]	0.461	0.285
Density [g/cm^3]	7.19	6.56
Crystal structure	bcc	hcp<~800°C < hcp + bcc<~1000°C < bcc
Thermal σ_a [barn]	3.1	0.2

Table 2
CS process conditions used to deposit Cr on Zircaloy-4.

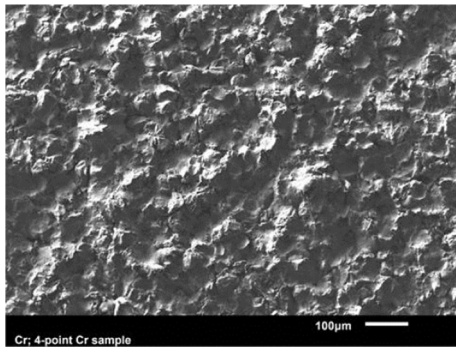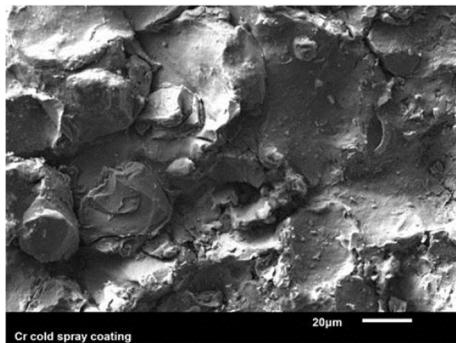|	
Nozzle type	WC-0.068
Carrier gas	Helium
Helium pressure [bar]	31.5
Preheater set point [°C]	700
Feeder set point	4
Standoff [inches]	1
Prechamber [inches]	3.5
Carrier gas flow [m^3/hr]	94
Helium flow [m^3/hr]	1319
Gun heater set point [°C]	675
Number of cycles	.25 (1 pass)
Gun speed [mm/s]	200

Fig. 2. As-coated sample.

Fig. 3. As-coated sample surface (higher magnification).

representativeness and duration of the experiment. The uncoated and coated samples were exposed to water steam at 500°C for more than 20 days. The flow rate varied between 8–11 g of water/min. According to previous studies, the 500°C steam oxidation should result in material corrosion that is very comparable with typical PWR irradiation–assisted corrosion [21].

2.2.1. Experimental setup

The setup consists of a big tank with deionized water heated by heat plates and a heat tape (steam generator). Steam coming from the steam generator is superheated in a furnace and piped away to the oxidation chamber. The chamber is heated by four independent heat tapes, ensuring uniform temperature inside the chamber. Several thermocouples monitor temperature distribution in the system and control the heat up and cooling of the system. The schematic representation of the setup is shown in Fig. 4.

2.3. High-temperature steam oxidation

2.3.1. Experimental setup

Cr-coated closed samples were oxidized in steam at 1200°C. The steam oxidation facility was designed to expose samples to flowing steam in a vertical tube over a range of temperatures (1000–1600°C) and steam flow velocities (1–9 m/s) at atmospheric pressure. The schematic representation of the setup used is shown in Fig. 4.

The Zry-4 tube was closed by an end plug also made from Zry-4 and welded by an electron beam. The tube was then polished, cleaned, coated with chromium by the CS, and oxidized in three consequent runs. First and second steam oxidations were 15 min long, and the last run was 60 min long. All tests were performed with the mass flow rate of 5.5 g/min, corresponding to a 2.19 m/s steam velocity and 0.032 $g/s.cm^2$ mass flux. Each sample was quenched in the air between each run. Only the first 6–7 cm of the rod is expected to be exposed to 1200°C steam because of the height limitation of the furnace.

2.4. Pressurization test

The oxidation facilities are designed to prove that the coating is protective in accident conditions and that it can reduce corrosion and related effects during normal operation. One of the main concerns of multicomponent claddings is adhesion of the coating
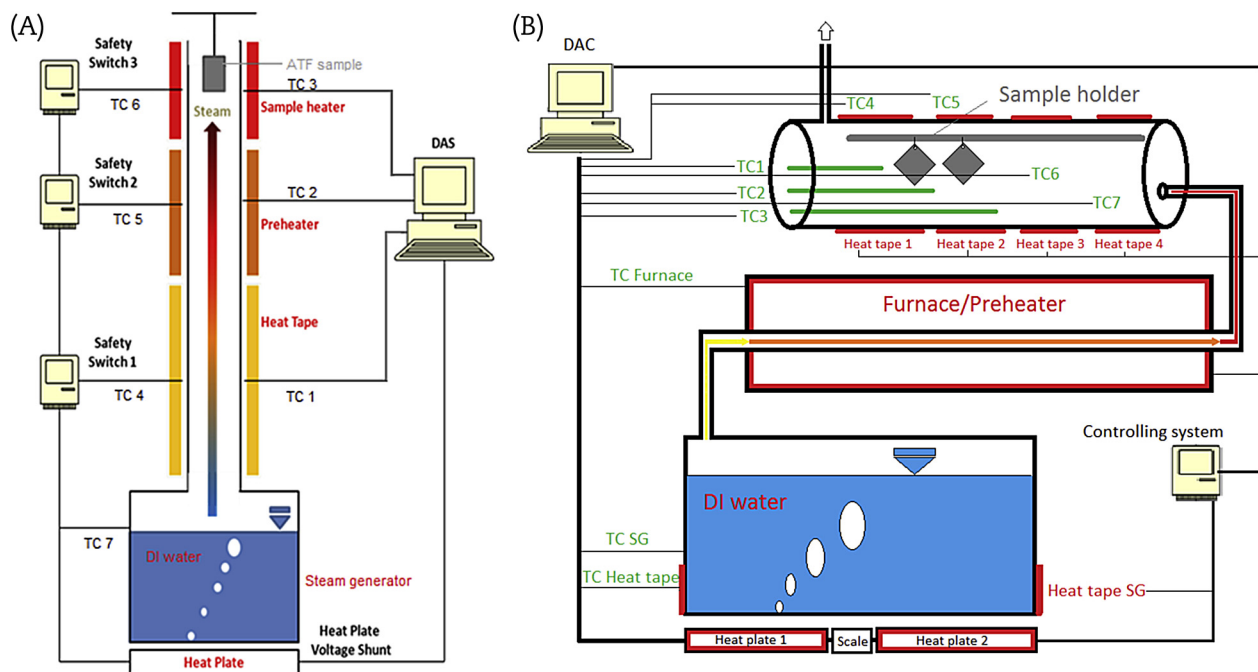

Fig. 4. Experimental setup. (A) Experimental setup for high-temperature testing. (B) Experimental setup for testing in 500°C steam. TC, thermocouple; DAS/DAC, data acquisition system/computer; ATF, accident-tolerant fuel; DI, deionized; SG, steam generator.

material during reactor operation. Fuel cladding undergoes various mechanical (both plastic and elastic) effects during normal operation, including creep, pellet-cladding mechanical interaction (PCMI), etc. Therefore, to demonstrate that it can serve its primary purpose as a protective layer, testing is necessary to determine if the coating survives such conditions.

2.4.1. Experimental setup

The pressurization test was designed to show the good adhesion properties of CS coatings in PWR conditions. The Zry-4 samples were first welded, then coated with chromium, and later inserted into a dynamic autoclave, which simulated in-reactor conditions with pressure of around 14 MPa and temperature of 310°C. Pure low conductivity water (0.05–0.08 μS/m) was used without any additions, and pH, inlet and outlet water conductivity, oxygen concentration, and electrochemical potential were monitored. The samples were open, with atmospheric pressure inside the tubes simulating open-gap condition.

After 20 days of compression of the cladding, the samples were pressurized up to 38 MPa for 12 days using argon to simulate PCMI conditions. Samples were then characterized, and the adhesion of the coating was studied. The appearance of uncoated and Cr-coated samples before, during, and after the pressurization test is shown in Table 3.

3. Results

3.1. 500°C steam oxidation

Two Cr-coated samples, two Cr metal samples, and four Zry-4 samples were oxidized in 500°C steam for up to 20 days. The Zry-4 corrosion shows very good agreement with published results, and oxide appearance and periodicity are similar to those after in-reactor irradiation-assisted corrosion. A correlation for Zry-4 corrosion was derived and was later used to precisely calculate the weight gains from areas of other samples that were not coated.

One side of the Cr-coated sample contained visible defects after fabrication, and the thickness of the coating was considerably lower. The CS coating is very nonuniform in comparison with alternative coatings, such as PVD or 3-D laser coatings, as can be seen in Fig. 5. However, the quality and also the uniformity of the coating can be improved by using finer particles and postspraying

treatment. Even with defects and nonuniform coating, the samples show very high corrosion resistance. The appearance of the samples during the test is summarized in Table 4. The pure chromium metal shows extraordinary oxidation resistance, and its weight gain is almost negligible. The weight gain of Cr-coated samples is higher due to defects that were found on all coated surfaces. It has to be noted that the weight gain of Cr-coated samples does not account for the surface roughness of the coating, which is high and considerably increases the oxidized area.

The scanning electron microscopy micrographs in Fig. 5 clearly show the different behaviors of Cr-coated and noncoated materials. The thickness of the Zr oxide at the edge of the sample reached 55 microns, whereas the Cr-coated surfaces show limited oxidation of the coating and the substrate. It can also be seen that Zr oxide is fragile and susceptible to cracking. The chromium coating remains stable even with low thickness and clearly protects the Zr-based substrate from oxidation in steam.

The graphs in Fig. 6 provide a comparison between the weight gains of pure Cr metal, Cr-coated Zry-4, and uncoated Zry-4. The weight gain of Zry-4 reaches almost 600 mg/dm^2 after 20 days, whereas the Cr-coated sample has a weight gain of around 95 mg/dm^2, and pure Cr metal has a weight gain of only 2.4 mg/dm^2. There is clear acceleration of oxidation kinetics in the case of Zry-4 after about 150 h, which is typical behavior for Zr–Sn binary alloys.

3.2. High-temperature steam oxidation

The sample was oxidized three times in sequence at 1200C. During the last run, the sample cracked, as can be seen in Fig. 8. The bottom end cap was made from a bulk Zry-4 material with different crystal orientation in comparison with the tubular section of the sample. It was hypothesized that due to the anisotropic thermal expansion coefficient of Zry-4, the excessive expansion of the end cap caused cracking of the sample. Defects from the CS process near the end cap could also have resulted in initiation of cracking. The end cap and different sections of the tubular sample were later analyzed.

Fig. 8 shows the appearance of the Cr-coated sample before and during oxidation. The appearance of the surface changed during the test in a manner similar to that of samples oxidized at 500°C (Table 4), from as-received silver color over blue and green thin layer of Cr oxide to brown/dark yellow color at the end of the test.

Table 3
Appearance of uncoated and Cr-coated samples during pressurization test.

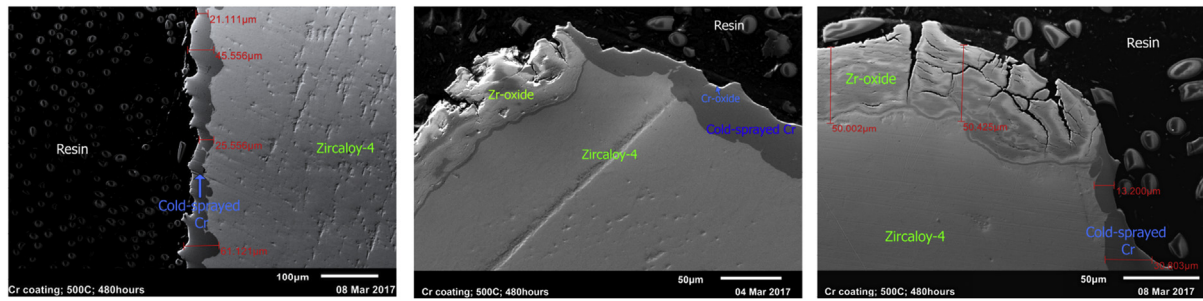| Sample condition	Cr coating	Zircaloy-4
As-received		
20 days compression		
12 days expansion		

Fig. 5. SEM micrographs of Cr-coated samples after 20 days of oxidation in 500°C. (A) - middle section of the coated coupon, Cr coating in non-uniform but very stable and protective, (B) The transition between coated and uncoated section of the coupon. Coating is adherent also on the Zr-oxide, (C) Direct comparison between coated and uncoated part of the sample with resulting oxide thicknesses after oxidation in 500°C steam.
SEM, scanning electron microscopy.

Table 4
Weight gains and appearances of the oxidation sample surfaces during the 500°C steam testing.

Exposition time		Zircaloy-4	Cr cold spray coating	Cr metal
1 day	Appearance			
	Weight gain [mg/dm^2]	**72.92**	**11.69**	**0.83**
4.3 days	Appearance			
	Weight gain [mg/dm^2]	**122.74**	**21.21**	**1.56**
11.6 days	Appearance			
	Weight gain [mg/dm^2]	**320.66**	**51.75**	**2.29**
20 days	Appearance			
	Weight gain [mg/dm^2]	**586.56**	**94.18**	**2.43**

Scanning electron microscopy micrographs show that the tube cracked after approximately 45 min of the last exposition. This was revealed based on the thickness of the inner oxide of the sample, calculated by the Cathart-Pawel correlation [22]. The outer Cr-coated surface of the sample proved to be very protective at high-temperature conditions even with very low thicknesses of the coating layer. As can be seen in Fig. 7, a coating layer thickness ranging between 3 μm and 20 μm successfully limited oxidation of the substrate.

The inner surface of the sample was exposed to steam for about 15 min, resulting in a 96-μm–thick Zr oxide. On the other hand, the outer surface was exposed to 15 + 15+60 min of high-temperature steam conditions, resulting in oxide which is 2–5 microns thick. This result is in agreement with the results of high-temperature testing of Cr-coated tubes performed by other groups [5], [13].

The end cap, which caused the cracking of the tube, showed completely different oxidation behavior in comparison with the tubular section of the sample. The chromium coating was still present, but a thick oxide layer was found underneath. The Cr coating was probably damaged at the tip of the end cap and steam oxidized the substrate under the coating, in effect causing two-sided oxidation. The elemental EDX summary of the end cap section is listed in Table 5. It needs to be pointed out that the atomic composition is only semiquantitative and should be used to understand the fundamental oxidation behavior, not to quantify the exact composition. The sample was very fragile due to the excessive oxidation, and some Cr layers may have been destroyed during cutting and handling.

3.3. Nanoindentation

One of the Cr-coated steam oxidation samples was used for nanoindentation test after oxidation in 500°C steam for 20 days. The test was performed at the interface between the Cr coating and
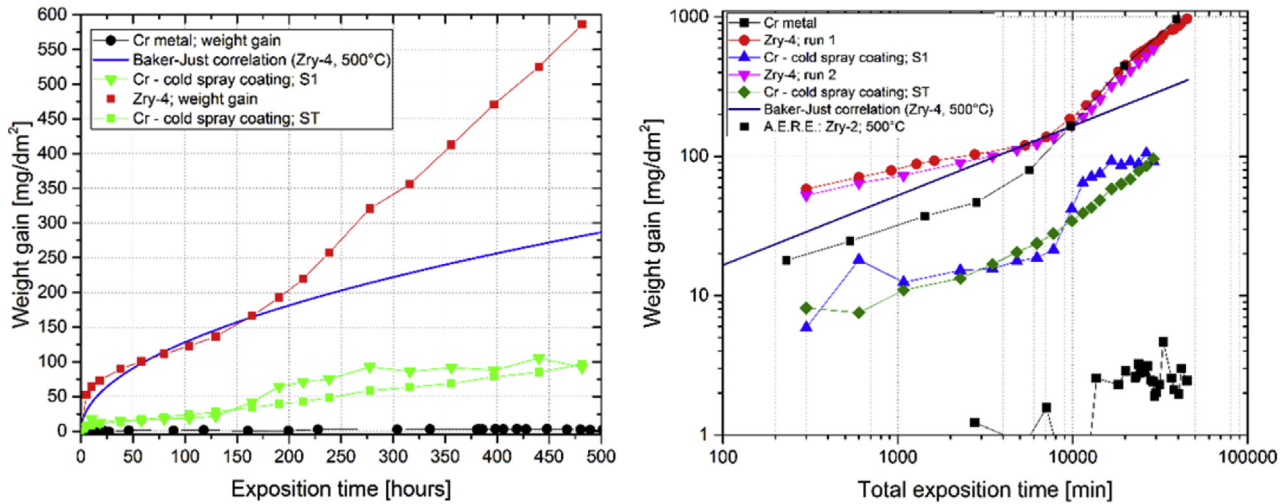
Fig. 6. Oxidation kinetics of Zry-4, Cr-coated samples, and pure Cr sample at 500°C steam. ST - testing sample where defects were observed on one side of the coated sample; S1 - sample with a high-quality coating on both sides of the coupon. (A) Weight gain as a function of time inside the oxidation chamber for Zry-4, Cr-coated samples, and pure chromium. There is a transition in oxidation kinetics visible in case of Zircaloy-4 after about 150 hours. (B) Oxidation kinetics of tested samples at 500°C steam compare to the B-J correlation and oxidation of Zircaloy-2.
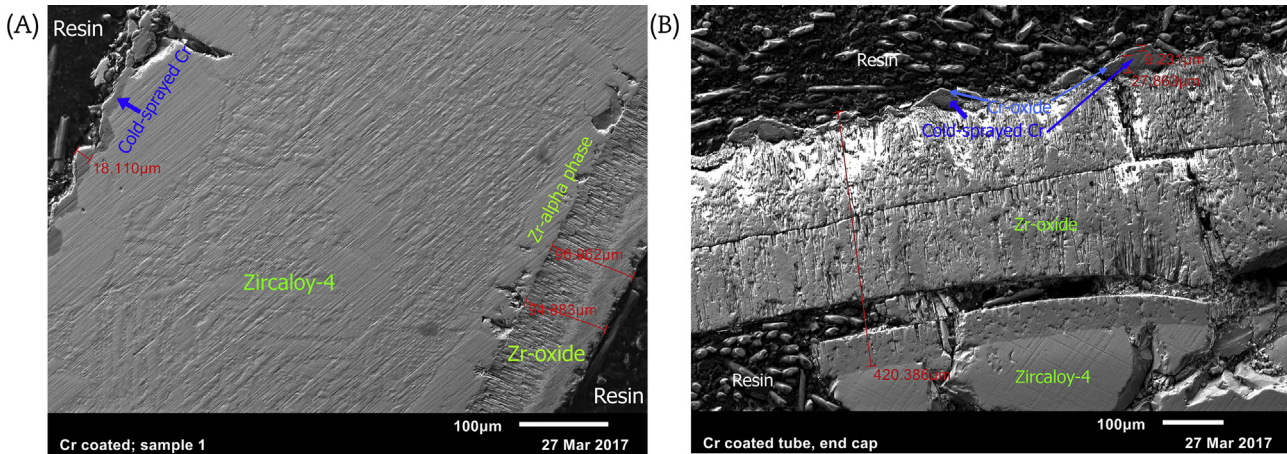

Fig. 7. SEM micrograps of different sections of Cr-coated sample oxidize at 1200°C steam. (A) Tubular part of Cr-coated sample after oxidation test. Inner Zr-oxide and oxygen-rich alpha phase are results of the inner oxidation after the end cap caused cracking. (B) Cr-coated end cap after high-temperature oxidation. The sample material is fragile but the coating is still adherent.
SEM, scanning electron microscopy.
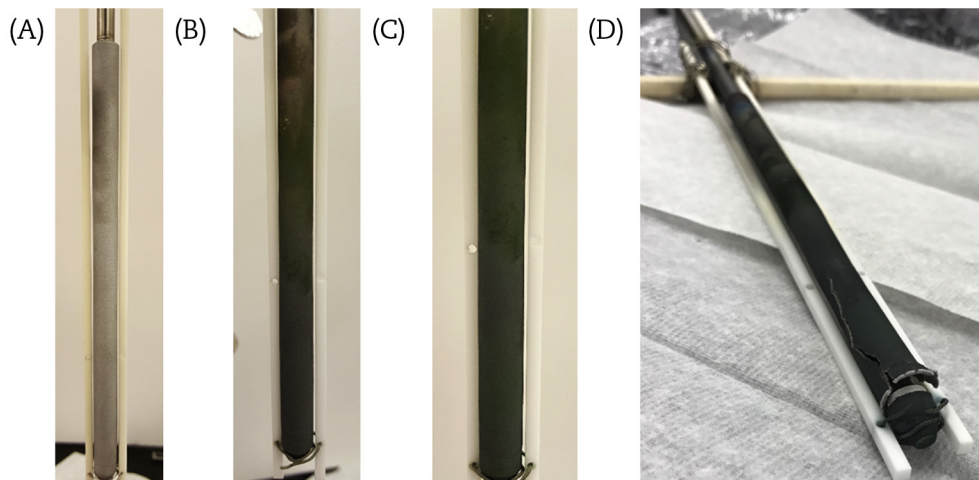

Fig. 8. Appearance of the Cr-coated sample during the high-temperature oxidation test. (A) Before the test. (B) After first 15 min steam exposition. (C) After second 15 min steam exposition. (D) After final 60 min steam exposition.

Table 5
Atomic composition of the end cap after high-temperature oxidation as measured by EDX using JEOL JSM 6610LS. The location of the point is shown in Fig. 9.

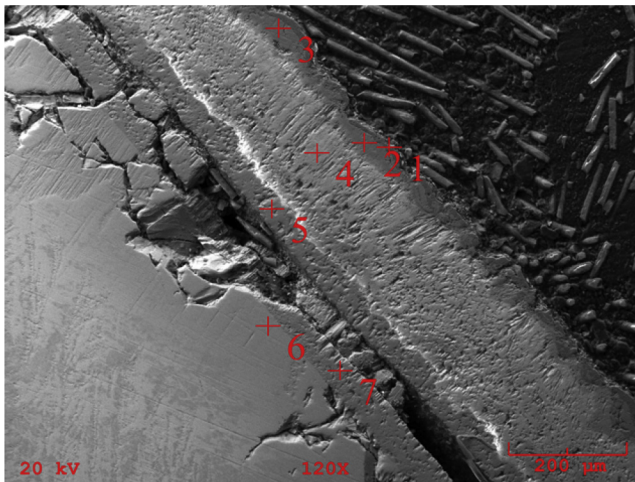| Element	Point #1	Point #2	Point #3	Point #4	Point #5	Point #6	Point #7
Zr [at. %]	0.2	8.9	1.1	41.7	44.9	71	42
O [at. %]	67.5	43.3	34.3	58.2	55	20.4	58
Cr [at. %]	32.2	47.9	64.6	0.1	0.1	8.5	0

Fig. 9. Cr-coated end cap after high-temperature oxidation.

the substrate, as can be seen in Fig. 10. The resulting average values are summarized in Table 6. The increase of the hardness at the interface between substrate and deposition material was observed earlier; it is caused by the interaction of sprayed particles with very high kinetic energy and Zry-4, causing a "cold work–like" effect.

A thin transition layer formed between the substrate and the Cr coating, affecting the material properties at the interface. The hardening effect can also be detected with soft coating materials. It is therefore hypothesized that the hardening effect is caused by the deposition process, not by the formation of the interlayer. Further investigations are, however, needed.
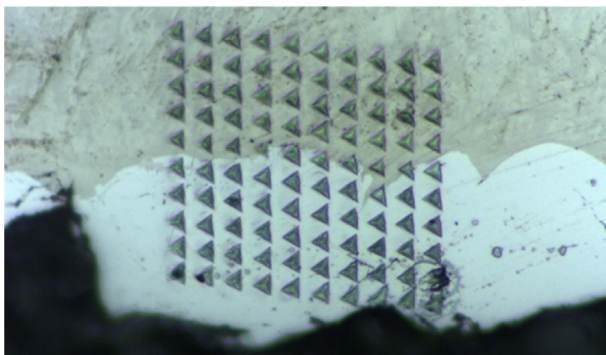

Fig. 10. Oxidized Cr-coated sample after nanoindentation.

Table 6
Results of nanoindentation at the interface-oxidized Cr/Zry-4.

Material	Reduced modulus [GPa]	Hardness [GPa]
Zircaloy-4	119.6 ± 12.2	4.06 ± 0.48
Interface Cr/Zr-4	171.8 ± 23.8	6.99 ± 1.72
Cold sprayed Cr	233.6 ± 26.4	5.02 ± 0.83

3.4. Fuel performance modeling

Preliminary fuel performance simulations have been performed using the finite element–based fuel performance code BISON [23]. The base cladding is modeled as Zr-4; its thermo-mechanical properties are detailed in BISON's theory manual [24]. As for the coating, chromium's thermo-mechanical properties had to be added to BISON. Specific heat, thermal conductivity, thermal expansion coefficient, Poisson's ratio, and yield strength were adopted from Holzwarth et al. [10]; temperature-dependent elastic modulus was adopted from Armstrong et al. [25]. Thermal creep is modeled using Norton's creep law from data published by Stephens et al. [11]. The yield strength is kept constant and is calculated as a function of temperature, with no strain or irradiation hardening. This is for preliminary probing and helps provide an upper bound for possible plastic deformation as no hardening is assumed.

As for the simulation run, a simplified PWR power history is used with a constant power of 18 kW/m and a standard cosine peaking factor, reaching an average burnup of around 60 MWd/kgU. A coating thickness of 50 μm is used for this simulation; the thickness is deducted from the base Zr cladding for the Zr-Ref and Zr–Cr to yield the exact same cladding dimensions. The resulting displacements, stresses, and plastic strains are shown in Fig. 11. The theoretical 50-μm–thick coating was chosen to ensure full coverage of the coating after undergoing wear in the LWR environment. The 50-μm Cr coatings on the fuel rods and guide tubes can introduce up to a 0.2% increase in enrichment requirement. The final thickness of the coating needs to be further optimized and is under investigation.

The Zr–Cr cladding showed performance similar to that of the reference Zry-4 cladding. The only differences came from the slightly lower inward creep for Zr–Cr; this resulted in delayed contact and smaller radial displacement by the end of life. Differences in fission gas release and consequent plenum pressure between the reference and the Cr-coated cases were within a range of ~3% of difference. Similarly, the fuel centerline temperature difference was less than ~2% in the precontact region due to the delayed gap closure for the Zr–Cr case. The chromium layer is expected to undergo plasticity during normal operation; this has not been experimentally confirmed to date. In this simplified case, the plastic deformation of the coating reached approximately 1% at the end of the simulated in-reactor life. Initial plasticity of the coating results from different thermal expansion coefficients; subsequent plasticity is mainly due to different creep and swelling strains between the two materials [26]. Based on preliminary calculations, the Cr CS concept is promising from the point of expected stress and strains during normal operation of PWRs. However, the simulation is based on available data, which to date are limited. The geometry and other operational parameters were simplified. Therefore, additional simulations and modifications of models are needed to precisely predict the behavior of Cr-coated nuclear cladding under more realistic operation conditions and possible transients, such as power ramps and loss-of-coolant accident (LOCA).

4. Discussion

The performance of cold sprayed Cr-coated Zry-4 cladding was presented. As supported by previous studies using PVD, Cr provides a better high-temperature oxidation resistant layer than does Zry-4. The coating exhibited good bonding strength and corrosion resistance even though standard commercial-grade powder and machinery with no postfabrication surface treatment were utilized. Compared with other deposition techniques (laser, and PVD), the coating is more heterogeneous and nonuniform due to the specifics of the CS technique. However, CS has advantages of high deposition
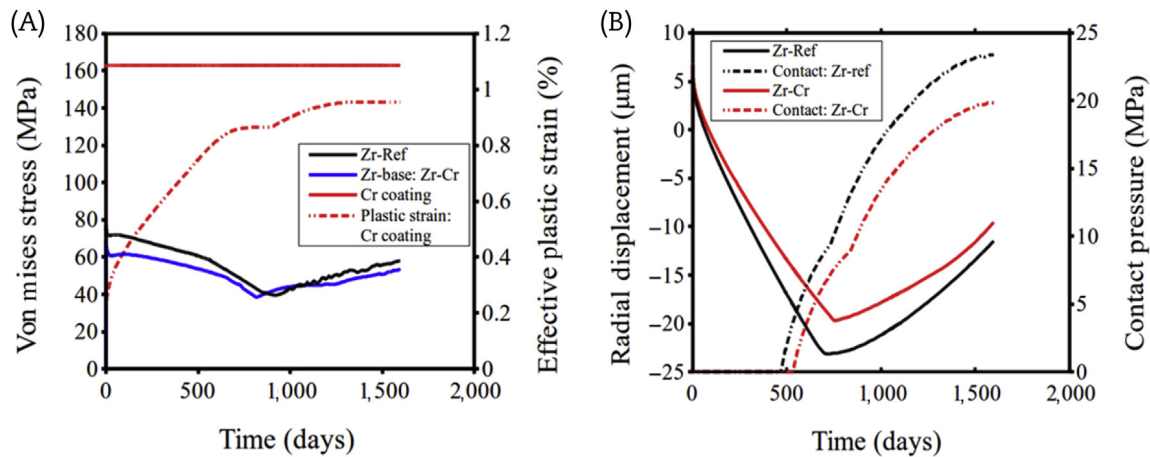
Fig. 11. Comparison between fuel performance characteristics of reference uncoated Zry-4 and Cr-coated cladding using BISON code. (A) Von mises stress and effective plastic strain as a function of time for reference uncoated case and two components of Cr-coted cladding. (B) Radial displacement of the cladding and contact pressure between fuel pellet and cladding as a function of time for reference uncoated case and two components of Cr-coated cladding.

rate and related commercial adoption by the industry. The simulation of the coated Cr cladding under steady state showed the small impact on the overall performance of the cladding and the feasibility of the concepts. Future work includes further testing, including testing under irradiation, model development, and assessment of the coating performance under accident scenarios.

Conflicts of interest

None declare.

Acknowledgments

References

[1] J.C. Brachet, C. Lorrette, A. Michaux, C. Sauder, I. Idarraga-Trujillo, M. Le Saux, M. Le Flem, F. Schuster, A. Billard, E. Monsifrot, E. Torres, F. Rebillat, J. Bischoff, A. Ambard, CEA studies on advanced nuclear fuel claddings for enhanced accident tolerant LWRs fuel (LOCA and beyond LOCA conditions), in: Fontevraud 8: Conference on Contribution of Materials Investigations and Operating Experience to LWRs' Safety, Performance and Reliability; Avignon (France), 2015, 15–18 Sep 2014; 15 refs, 32 p.

[2] H.-G. Kim, J.-H. Yang, W.-J. Kim, Y.-H. Koo, Development status of accident-tolerant fuel for light water reactors in Korea, Nucl. Eng. Technol. 48 (1) (Feb. 2016) 1–15.

[3] B. Maier, et al., Development of cold spray coatings for accident-tolerant fuel cladding in light water reactors, JOM 70 (2) (2018).

[4] J. Krejci, M. Sevecek, L. Cvrcek, Development of chromium and chromium nitride coated cladding for VVER reactors, in: Proceedings, WRFPM, 2017. A-131.

[5] A.S. Kuprin, et al., Vacuum-arc chromium-based coatings for protection of zirconium alloys from the high-temperature oxidation in air, J. Nucl. Mater. 465 (Oct. 2015) 400–406.

[6] R. Van Nieuwenhove, V. Andersson, J. Balak, B. Oberländer, In-pile testing of CrN, TiAlN and AlCrN coatings on Zircaloy cladding in the halden reactor, in: 18th International Symposium on Zirconium in the Nuclear Industry, 2016.

[7] K. Daub, R. Van Nieuwenhove, H. Nordin, Investigation of the impact of coatings on corrosion and hydrogen uptake of Zircaloy-4, J. Nucl. Mater. 467 (Dec. 2015) 260–270.

[8] ASTM International, ASTM B614–b616 Standard Practice for Descaling and Cleaning Zirconium and Zirconium Alloy Surfaces, West Conshohocken, PA, 2016.

[9] C.W. Weaver, Irradiation and the ductility of chromium, Scr. Metall. 2 (8) (Aug. 1968) 463–466.

[10] U. Holzwarth, H. Stamm, Mechanical and thermomechanical properties of commercially pure chromium and chromium alloys, J. Nucl. Mater. 300 (2) (2002) 161–177.

[11] J.R. Stephens, W.D. Klopp, High-temperature creep of polycrystalline chromium, J. Common Met. 27 (1) (1972) 87–94.

[12] I. Idarraga-Trujillo, et al., Assessment at CEA of coated nuclear fuel cladding for LWRS with increased margins in LOCA and beyond LOCA conditions, in: Conference Paper LWR Fuel Performance Meeting, Top Fuel 2013, vol. 2, 2013, pp. 860–867.

[13] H.-G. Kim, I.-H. Kim, Y.-I. Jung, D.-J. Park, J.-Y. Park, Y.-H. Koo, Adhesion property and high-temperature oxidation behavior of Cr-coated Zircaloy-4 cladding tube prepared by 3D laser coating, J. Nucl. Mater. 465 (Oct. 2015) 531–539.

[14] R. Tucker Jr., Thermal spray technology, ASM Handbook, Volume 5A, Plast. Ind. 335 (2013) 336.

[15] V.K. Champagne, D. Helfritch, P. Leyman, S. Grendahl, B. Klotz, Interface material mixing formed by the deposition of copper on aluminum by means of the cold spray process, J. Therm. Spray Technol. 14 (3) (Sep. 2005) 330–334.

[16] M. Hassani-Gangaraj, D. Veysset, K.A. Nelson, C.A. Schuh, Supersonic impact of metallic micro-particles, in: Proceedings of the 2006 ITSC, ASM, Seattle, 2016. ArXiv161208081.

[17] T. Stoltenhoff, F. Zimmermann, LOXPlate® coatings for aluminum aerospace components exposed to high dynamic stresses, Praxair Surface Technologies GmbH, Ratingen, Germany, 2012.

[18] R. Maev, V. Leshchynsky, A. Papyrin, Structure formation of Ni-based composite coatings during low pressure gas dynamic spraying, in: Proceedings of the 2006 International Thermal Spray Conference, 2006.

[19] N. Bay, Cold Welding. Part 1: Characteristics, Bonding Mechanisms, Bond Strength, 1986.

[20] J. Vlcek, L. Gimeno, H. Huber, E. Lugscheider, A systematic approach to material eligibility for the cold-spray process, J. Therm. Spray Technol. 14 (1) (2005) 125–133.

[21] C. Duriez, T. Dupont, B. Schmet, F. Enoch, Zircaloy-4 and M5® high temperature oxidation and nitriding in air, J. Nucl. Mater. 380 (1–3) (Oct. 2008) 30–45.

[22] R.E. Pawel, J.V. Cathcart, R.A. McKee, The kinetics of oxidation of Zircaloy-4 in steam at high temperatures, J. Electrochem. Soc. 126 (7) (Jul. 1979) 1105–1111.

[23] R.L. Williamson, et al., Multidimensional multiphysics simulation of nuclear fuel behavior, J. Nucl. Mater. 423 (1–3) (Apr. 2012) 149–163.

[24] J. Hales, et al., BISON Theory Manual the Equations behind Nuclear Fuel Analysis, Idaho National Laboratory (INL), Idaho Falls, ID (United States), 2016.

[25] P.E. Armstrong, H.L. Brown, Dynamic Young's modulus measurements above 1000 C on some pure polycrystalline metals and commercial graphites, Trans. Aime 230 (1964) no. LADC-6100.

[26] M. Wagih, Y. Che, K. Shirvan, Fuel performance of multi-layered zirconium based accident tolerant fuel cladding, in: ICAPP, 2017.